

УДК 539.165

MEASUREMENTS OF THE ^{187}Re BETA SPECTRUM

P.Valko, M.R.Gomes, T.A.Girard

Centro de Fisica Nuclear, Universidade de Lisboa, 1649-003 Lisboa, Portugal

Motivation for precise beta spectrum measurements of ^{187}Re decay and currently used experimental methods are presented. Possible novel methods of beta spectroscopy based on magnetically induced metastable superconducting systems are also discussed.

В работе представлены обоснование прецизионного измерения бета-спектра ^{187}Re и используемая экспериментальная методика. Обсуждаются принципиально новые методы бета-спектроскопии, основанные на использовании магнитно-индуцированных метастабильных сверхпроводящих систем.

INTRODUCTION

Neutrinos are currently the most mysterious elementary particles for whose existence we have direct experimental evidence. The fact that they interact only via weak and weaker (supersymmetric, gravitational) interactions makes difficult their study with the precision we would like. Although we have experimental observation of neutrino existence, and properties [1], the most important property – the mass – is still unknown. Based on current understanding of the universe evolution, the neutrino abundance can be compared only with the cosmic microwave background photon abundance, i.e., they are the second most common particles in the universe. This makes the rest mass of neutrinos one of the most important parameters for modern cosmology.

All the current experiments which are able to derive information about neutrino mass have produced only upper limits, with the best model-dependent values coming from indirect searches based on double beta decay data and neutrino mixing searches [2,3]. The best direct limit on electron neutrino mass, derived from measurements of the tritium decay spectrum near end point, is $2.5 \text{ eV}/c^2$ at 95 % C.L. [4]; all measurements observe the so-called end-point anomaly ($m_\nu^2 < 0$), however [5]. The enormous experimental difficulties associated with large electromagnetic beta spectrometers, especially the problem of intense source preparation and characterization, make further improvement of the current limit very difficult. In this respect the possible positive observation of neutrino mass in tritium might be challenged with several side-effect explanations, and an alternative direct experiment in other materials is therefore very important.

There is no large list of low-energy beta decays which could be used in a direct electron antineutrino mass search. Besides ^3H , only a few other isotopes with sufficient low transition energy and other decay properties (to the ground state) could be potentially used. From possible candidates such as ^{63}Ni , ^{107}Pd , ^{187}Re has the lowest transition energy. The good statistics of the spectrum measured near end point is the most important aspect of neutrino mass limit derivations. The lower transition energy means a larger fraction (f) of counts in

the same energy band: for ^{187}Re , $f = 10^{-4}$ for 10 eV below end point, vs. 10^{-7} in the case of tritium. This makes ^{187}Re a natural candidate for a direct neutrino mass experiment. Rhenium-187 is an isotope with a natural 62.6 % abundance. The decay lifetime is $4.35 \cdot 10^{10}$ years with $Q_{\beta^-} = 2.663$ keV and transition is first unique-forbidden ($5/2^+$ to $1/2^-$). The Genoa Group [6] and more recently Milan [7] have pursued successfully the measurement of ^{187}Re decay using cryogenic μ -calorimeters.

1. CRYOGENIC DETECTORS

To address the count-rate limitation of electromagnetic spectrometers due to the internal source absorption, the detector system in which the source is an integral, sensitive part itself should be used. Such schemes are possible in various cryogenic detector designs. There are several, sometimes significantly different, ways to achieve the required detector sensitivity. The current field of cryogenic detectors ranges from «simple» calorimeters, superconducting metastable systems, superconducting tunnel junctions, superconducting transition edge sensors to «exotic» superfluid ^3He detectors [8]. In this work, only the first two categories will be discussed.

1.1. Calorimetric Detectors. The general concept of phonon-mediated cryogenic detectors is to register temperature increase generated by energy deposition of a particle passing through (stopped in) an absorbing material. A schematic of such a detector is shown in Fig. 1. When

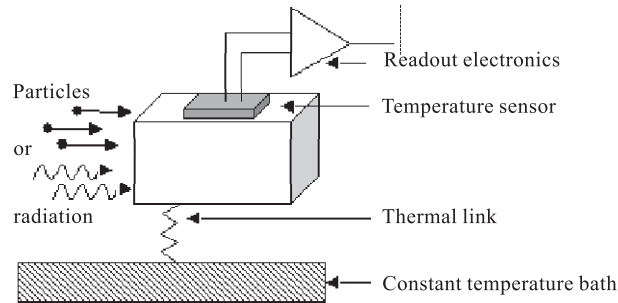


Fig. 1. Basic scheme of a calorimetric detector

the energy E is absorbed and distributed among possible excitations (phonons) for a given material and temperature (full thermalization), the measured temperature rise ΔT is given as

$$\Delta T = \frac{E}{c(T)}, \quad (1)$$

where $c(T)$ is the total (effective) heat capacity of the detector at temperature T . At low temperatures, a very small heat capacity can be achieved with pure dielectric crystal and superconductor absorbers due to the strong decrease of their specific heat with decreasing temperature. For a dielectric crystal, only the specific heat of the lattice contributes and the

molar value is given as

$$c_{\text{dielectric}} = 234N_A k_B \left(\frac{T}{\Theta_D} \right)^3, \quad (2)$$

where N_A is Avogadro's number and Θ_D is the Debye temperature of the crystal. In the case of a superconductor, the electron specific heat decays exponentially for temperatures below T_c . The superconducting absorber heat capacity is therefore given as

$$c_s = 234N_A k_B \left(\frac{T}{\Theta_D} \right)^3 + \alpha e^{-(\beta\Delta/k_B T)}, \quad (3)$$

where Δ is the superconductor energy gap value and α, β are material parameters. The energy resolution is limited by thermodynamical fluctuations of the detector owing to the random exchange of phonons through the thermal link, and can be expressed as

$$\Delta E = \epsilon \sqrt{k_B T^2 C}, \quad (4)$$

where ϵ is a factor determined by the temperature sensitivity of the thermometer. The typical temperature sensors implemented in current cryogenic calorimeters are nuclear (neutron) transmutation doped (NTD) germanium and silicon ion implanted thermistors [9].

1.2. The Geometrically Metastable Superconducting Detector. The superconducting metastable systems were historically one of the first cryogenic detectors proposed. The original idea was to utilize the fast transition from the superheated state of type-I superconducting spherical grains to the normal state in external magnetic field. Geometrical metastability is similar in its basic underlying physics, although the response of the detector system is significantly different. The $S \rightarrow N$ phase transition of a type-I superconducting foil in a perpendicular magnetic field is initiated when the field at the foil edge reaches the thermodynamic critical field (H_c). This occurs when the applied field strength (H_{fp}) is well below H_c , owing to the geometry-dependent demagnetization of the foil [10].

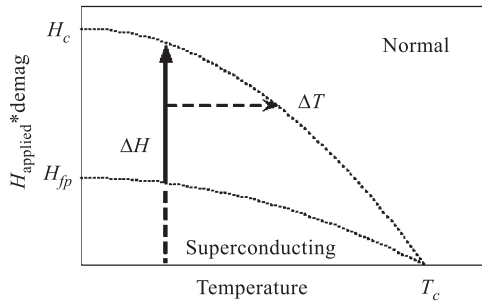


Fig. 2. Phase diagram of a geometrically metastable superconducting strip in a perpendicular magnetic field

Meissner effect are detected to yield the interaction signal. The signal is then generally composed of two distinct contributions; these can be resolved by the insertion of a pause during the field increase, which yields the signal profile shown in Fig.3. This can be «deconstructed» by $S(t) = S_M + S_T$, with

The flux is driven to the center by Gibb's free energy potential, lowering the edge field and requiring increase of the applied field to generate further flux entry. In consequence, the transition is delayed over a large ΔH , and the foil is generally in an intermediate (or mixed) state. During the phase transition, local heating generated by energy deposition of incident radiation can nucleate the normal state if the temperature increase (ΔT) is sufficient to raise the temperature above the phase line as shown in Fig. 2.

Pulses induced in a surrounding loop by the flux changes associated with the loss of the

$$S_j(t) = s_j(1 - e^{-(t/\tau_j)}), \quad (5)$$

where the first term corresponds to the magnetic contribution, and the second to the thermal one. Fitting of the data typically yields $\tau_M = 0.29 \pm 0.06$ s, corresponding to the effective damping constant of the magnet and induced currents in the cryostat materials. The saturation of the curve implies a time-dependent measurement efficiency (ρ), which can be expressed as

$$\rho(t) = \frac{s_T}{S_0} [1 - \tau_T(\Delta t)^{-1} \times (1 - e^{-(\Delta t/\tau T)})], \quad (6)$$

where Δt is the pause time and S_0 is the source activity, yielding $\rho \sim 70\%$ with typical experimental values. In general, pulse height $= \partial\phi/\partial t \sim \int \mathbf{B} \cdot d\mathbf{S} = \mu_0 H_c S_\phi$, where S_ϕ is the surface area of the nucleated flux tube and flux variations are assumed to occur on superconducting time scales. Measurements of ^{109}Cd conversion electron irradiations of a tin device have shown the pulse-height to be linear with energy, such that $\Delta E/L_y S_\phi = \text{const.}$ [11]. Energy resolution is thus dependent on the variation of the penetrating flux size per event.

2. CALORIMETRIC RESULTS

The μ -calorimeter essentially consists of a thermistor mounted on a natural rhenium absorber, operated below ~ 100 mK. Since rhenium is a superconductor with $T_c = 1.7$ K

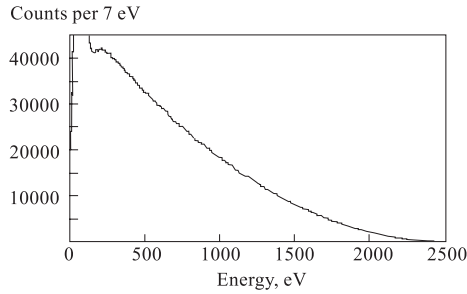


Fig. 4. ^{187}Re beta spectrum measured with 1.5 mg calorimeter [6]

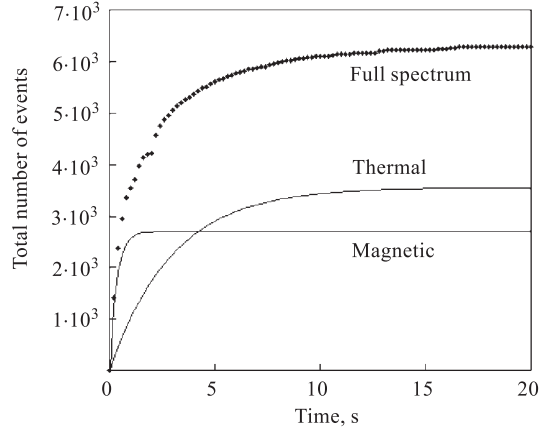


Fig. 3. A representative timing profile of flux penetration during a pause inserted in a field ramp

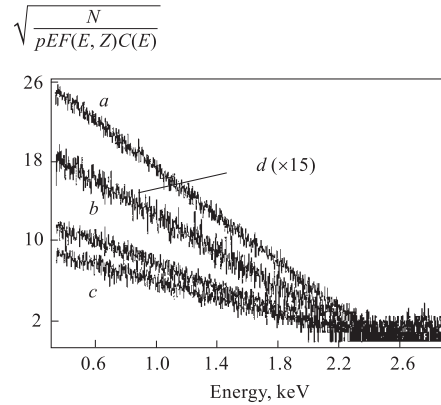


Fig. 5. ^{187}Re beta spectrum produced by 4 individual Si thermistor detectors with AgReO_4 absorbers identical to sources [7]

and $H_c(0) = 210$ G, the Genoa Group measurements make use of the reduced specific heat of the superconducting material (Eq. 3, see Fig. 4), while the Milan measurements are based on specific heat behavior (Eq. 2, see Fig. 5) of dielectric silver perrhenate (AgReO_4) crystals. Results to date impressively demonstrate a full undistorted decay spectrum down to 100 eV, with a resolution of ~ 13 eV at 5.9 keV. The timing resolution is however of order 10 ms, so that these measurements are statistically limited by pileup considerations to a rate of a few Hz. Neither group has yet produced a limit on the possible neutrino mass.

3. CURRENT STATUS OF METASTABLE RHENIUM DETECTOR

We show in Fig. 6 a typical thermal-only component pulse height spectrum, displayed as the variation of $[\text{events}]^{1/2}$ with energy. This was obtained with a 99.99% pure, 25 μm

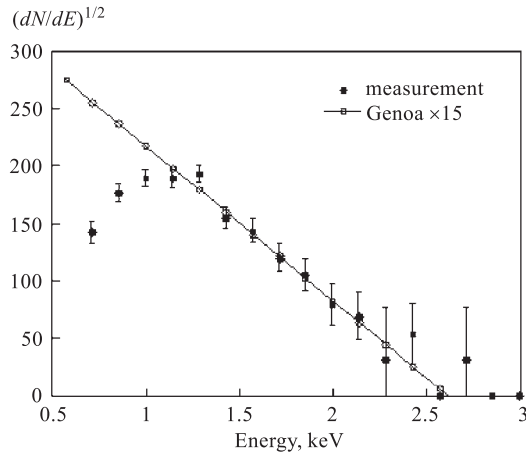


Fig. 6. Preliminary decay spectrum of ^{187}Re with magnetically metastable device

thick natural polycrystalline ribbon, with width and length 0.900 ± 0.030 and 15 ± 0.01 mm, respectively. The foil was zero field cooled to $T = 330 \pm 10$ mK; the field was then ramped from zero to 88 G at a rate of 16 G/s, stopped for 20 s, and then continued to 250 G, well above H_c (200 G), before being returned to zero. The noise limit in these measurements corresponds to flux tubes of $1140 \phi_0$. The integrated thermal rate is ~ 8.5 Hz over the pause period, comparable with the 12 Hz anticipated from the device size. The measured thermal spectrum is however a linear combination of radiation-stimulated events with genuine delayed magnetic penetration.

The timing resolution of the acquisition electronics is of order 10 μs , implying a

data acquisition rate more than 10 kHz. The intrinsic time scale of the penetration process is even faster (several tens of nanoseconds), as has been previously demonstrated [12], suggesting the ability to eventually accommodate event rates approximately 10^5 larger than the calorimeters.

The physics of magnetic flux penetration into 2D superconducting samples is on the edge of main-stream solid state physics interest [13], and a detailed solid state study of the relevant processes is needed. While these results are encouraging, we stress that the basic physics underlying the foil response to irradiation is not yet understood. Experiments in which the pause is inserted *below* H_{fp} in fact yield similar pulse height spectra with linear timing profiles. Although this is consistent with a recent description of explosive nucleation of the normal state with laser irradiation by Ghinovker et al. [14], the description neglects the geometric barrier and its influence on the signal response remains to be elaborated.

SUMMARY

Measurement of the decay spectrum of ^{187}Re provides an alternative means of establishing new limits on the electron antineutrino mass, and confirmation of the end-point anomaly observed in current tritium experiments.

Measurements of the Re decay spectrum in microcalorimeters demonstrate spectrum linearity and low baseline performance. They are however currently limited in statistical power. The main goal of the current activity is to establish the most effective method of absorber (source) and thermometer combination. For potential future large-scale experiments with few eV neutrino mass sensitivity, the optimal configuration with long-term stability, large source mass must be chosen.

Preliminary measurements of the decay of ^{187}Re in thin geometrically metastable foils appear to yield an electron spectrum with linear response down to ~ 1 keV. The current device is two orders of magnitude faster than calorimeters, and can in principle be improved by another three orders. Current noise level can be reduced by use of cooled, low-noise electronics or SQUID-based readout. Energy resolution in this device is predicated on the ability to resolve flux bundle size, which has been shown to be linear in the deposited energy [15]. Due to the quantum nature of magnetic flux, the fundamental energy resolution will be limited by a step of ϕ_0 in flux penetration.

Acknowledgements. We thank J.Collar, D.Limagne and G.Waysand of the Groupe de Physique des Solides, Universites Paris 7/6 for technical discussions, and C.Oliveira of ITN for MCNP simulations of the calibrations. This work was supported in part by grant CERN/FAE/1211/98, under the Ministry of Science & Technology of Portugal.

REFERENCES

1. Review of Particle Properties // Eur. Phys. J. C. 1998. V. 3. P. 1.
2. Ejiri H. // Neutrino 2000 Conf. <http://nu2000.sno.laurentian.ca>.
3. Lisi E. et al. // Neutrino 2000 Conf. <http://nu2000.sno.laurentian.ca>.
4. Lobashev V.M. et al. // Neutrino 2000 Conf. <http://nu2000.sno.laurentian.ca>.
5. Lobashev V.M. et al. // Nucl. Phys. B. 2000. V. 87. P. 275.
6. Gatti F. et al. // Nature. 1999. V. 397. P. 137.
7. Alessandrello A. et al. // Phys. Lett. B. 1999. V. 457. P. 253.
8. Twerenbold D. // Rep. Prog. Phys. 1996. V. 53. P. 349.
9. Alessandrello A. et al. // J. Phys. D. 1999. V. 32. P. 3099.
10. Castro H. et al. // Phys. Rev. B. 1999. V. 59. P. 596.
11. Judy V. et al. // Nucl. Instr. Meth. A. 1996. V. 370. P. 104.
12. Furlan M. et al. Low Temperature Detectors for Neutrinos and Dark Matter-III / Ed. Frontiers. Gif-sur-Yvette, 1991. P. 21.
13. Zeldov E. et al. // Phys. Rev. Lett. 1994. V. 73. P. 1428;
Zeldov E. et al. // Europhys. Lett. 1995. V. 30. P. 367.
14. Ghinovker M., Shapiro I., Shapiro B.Ya. // Phys. Rev. B. 1999. V. 59. P. 9514.
15. Judy V. et al. // Nucl. Instr. Meth. A. 1996. V. 373. P. 65.